IOP Conf. Series: Journal of Physics: Conf. Series **844** (2017) 012042 doi:10.1088/1742-6596/844/1/012042

Influence of Incident Polarization State on Performance of Real-time Transverse Force Sensing using Stokes Parameters in Fiber Bragg Grating

Yang Su*， Xinhao Fu, , Hua Zhou, Yong Zhu, Baofu Zhang, Guangyu Cai, and Yang Guo

Institute of Communications Engineering, PLA University of Science and Technology, Nanjing, China 210017
qieziyangyang@163.com

Abstract. Stokes parameters can be advantageously used to obtain real-time transverse force measurements with uniform FBGs. In this paper, we demonstrate here that the state of polarization (SOP) of incident light can be used to improve the performance of the sensor. The model and the simulations are presented. A 3-paddle fiber polarization controller was used to adjust the azimuth angle and ellipse angle of the light. The experimental results show the great influences of incident SOP on the sensitivity and linear range of the system, which is well agreed with the theoretical prediction. The highest sensitivity of 0.9475/kgf was obtained with good linearity.

1. Introduction

Fiber Bragg gratings (FBGs) are key components for both optical fiber telecommunications and sensing applications. While the most straightforward applications remain temperature and axial strain sensing, which changes the center wavelength of the reflected spectrum when the sensing parameters cause grating effective index or grating period variation [1–2]. In practice, the characteristics of a FBG under transverse load are quite different from axial load [3–4]. In the case of transverse load, stress induced birefringence effects will cause the unique Bragg grating condition to break down and even produce two distinct Bragg wavelengths [5,6].

However, this effect cannot be directly observed on the amplitude spectrum for limited load values (<1 N/mm)[7]. In the other hand, it has been demonstrated that the spectral response of the polarization dependent loss (PDL) [8] or the differential group delay (DGD) [9] is very sensitive to the birefringence within the grating, which can provide more effective information and therefore lead to the potential development of new types of FBG-based optical sensors [7–9] used to monitor weak transversal load. By measuring PDL or DGD peak amplitudes the amount of applied force is determined. Although the structure is simple, this design requires a complex measuring system to determine the peak values. Large amounts of data points over a wide range of spectrum must be continually analyzed in high resolution, resulting in a rather slow processing speed.

FBGs used as transversal load sensors can be applied in many domains such as structural health monitoring of composite materials [10–11] or for biomedical applications [12-13]. Therefore it is necessary to do research for real-time sensing. We have proposed a compact real-time transverse-force sensing system through Stokes parameters measurement at single wavelength [14]. The measuring system in our approach is simple and does not require processing of massive amount of spectral data,

Content from this work may be used under the terms of the Creative Commons Attribution 3.0 licence. Any further distribution of this work must maintain attribution to the author(s) and the title of the work, journal citation and DOI.
Published under licence by IOP Publishing Ltd

enabling real-time transverse force monitoring. The proportional relationship and linear fit can be observed between the applied force and the Stokes parameters from the FBG.

For practical applications, it is of high importance to have the possibility to improve the sensitivity and enlarge the linear range. In this paper we put emphasis on how to improve system performance. By simulations, it is demonstrated that the state of polarization (SOP) of incident light has great influence of on sensitivity and linearity of the sensor. A 3-paddle fiber polarization controller (PC) was used to modify the polarization state of the incident light in the experiment and the experimental data confirm the simulations well. In the experiment results, a highest sensitivity of 0.9475/kgf is gained with good linearity. Therefore, a simple method to improve sensor performance by adjusting incident SOP of light using PC is proposed in this paper.

2. Principle and simulations

When the FBG is subjected to a transverse load, the difference between the effective refractive indices of the two orthogonal modes of the fiber within the loaded region will be produced. For simplicity the direction of the transverse force is assumed as y (fast axis), another direction perpendicular to y-axis is x direction (slow axis), z is along the fiber axial direction, as shown in Fig. 1.

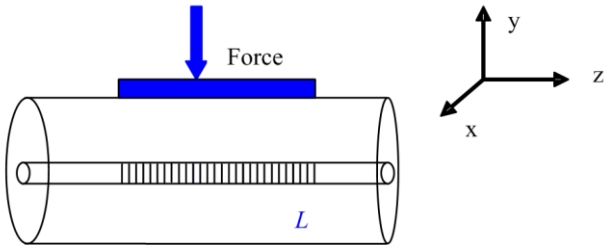

Fig. 1. Schematic showing the defined coordinate system.

The refractive index changes $\left(\Delta n_{eff}\right)_x$ and $\left(\Delta n_{eff}\right)_y$ within the loaded zone are given by[6,15]

$$\left(\Delta n_{eff}\right)_x = -\frac{n_{eff}^3}{2E}\left\{\left(p_{11}-2vp_{12}\right)\sigma_x + [(1-v)p_{12}-vp_{11}](\sigma_y+\sigma_z)\right\} \quad (1)$$

$$\left(\Delta n_{eff}\right)_y = -\frac{n_{eff}^3}{2E}\left\{\left(p_{11}-2vp_{12}\right)\sigma_y + [(1-v)p_{12}-vp_{11}](\sigma_x+\sigma_z)\right\} \quad (2)$$

Where E and v are the Young's modulus and Poisson's coefficient of the optical fiber respectively, p_{11} and p_{12} are the strain-optic coefficients. For typical optical fiber, E=74.52 GPa, v=0.17, p_{11} =0.121, and p_{12}=0.270. σ_x, σ_y and σ_z are the stress components in the grating in the x, y and z directions, respectively. They are expressed in the Hertz equations [5,6]:

$$\sigma_x = \frac{2F}{\pi DL};\quad \sigma_y = -\frac{6F}{\pi DL};\quad \sigma_z = u\cdot v(\sigma_x+\sigma_y) \quad (3)$$

Where D is the fiber diameter, F is the applied force, and L is the length of the region under stress, u is the correction coefficient which is related to the smoothness of the optical fiber and compression platform. The case of u = 0 denotes that the contact plane is perfectly smooth (no friction) and the fiber is in plane stress state (ends-free). In order to simplify the model of fiber stresses, we limit ourselves to this case.

The refractive indexes in the x and y-directions are then given by $n_{eff,x} = n_{eff} + (\Delta n_{eff})_x$ and $n_{eff,y} = n_{eff} + (\Delta n_{eff})_y$, respectively, with birefringence:

$$\Delta n = (\Delta n_{eff})_x - (\Delta n_{eff})_y \quad (4)$$

Due to Δn, the x and y modes undergo different couplings through the grating. The total transmitted signal is, therefore, the combination of the x and y mode signals. In a Cartesian coordinate system whose reference axes match the FBG eigenmodes, the Jones matrix of the grating is diagonal [8,9]:

$$J_{grating} = \begin{bmatrix} t_x & 0 \\ 0 & t_y \end{bmatrix} \tag{5}$$

In Eq. (5), $t_{x(y)}$ denotes the transmission coefficient of the FBG corresponding to the $x(y)$ mode [16].

The Stokes parameters represent the state of polarization. We firstly translate the Jones matrix of the grating to a 4×4 Muller matrix $M_{grating}$ and then get the Stokes vector of the transmitted signal $(S_0, S_1, S_2, S_3)_{out}^{\ T}$ by

$$\begin{pmatrix} S_0 \\ S_1 \\ S_2 \\ S_3 \end{pmatrix}_{out} = M_{grating} \begin{pmatrix} S_0 \\ S_1 \\ S_2 \\ S_3 \end{pmatrix}_{in} \tag{6}$$

Where $(S_0, S_1, S_2, S_3)_{in}^{\ T}$ represents the Stokes vector of incident light. It can be determined by two para meters, ie. ellipticity angles κ and azimuth angle θ, and therefore Stokes vector can be written as

$$(1, (\cos 2\kappa)(\cos 2\theta), (\cos 2\kappa)(\sin 2\theta), \sin 2\kappa)_{in}^{\ T} \tag{7}$$

Then the normalized Stokes parameters (s_1, s_2 and s_3) can be computed using:

$$s_i = S_i / S_0 \quad (i = 1, 2, 3) \tag{8}$$

So the relationship between transversal force and the normalized Stokes parameters are found using Eqs. (1)-(8) [19].

Simulated s_1, s_2 and s_3 spectrum evolutions for different values of birefringence are shown in [14] and the amplitude of Stokes parameters at single wavelength changes with increase of applied force. However the incident SOP will affect the response performance, which sometimes presents very low sensitivity. So how to find a solution to get a better response is important.

The changes of amplitude of Stokes parameters respect to applied force are studied. Simulated results for different κ with θ of 10 degree are shown in Fig. 2(a). And Fig.2 (b) shows simulated results for different θ with κ of 25 degree. From these results we can conclude that κ and θ has grate influence on the sensitivity and linear range of the system. And in some cases non-linearity is shown. So the choice of incident SOP is important. Maybe κ of 45° is a better choice. However we should realize that the simulations can not agree with experimental results exactly. That is because we can not control or get the accurate SOP of incident light due to the existence of fiber segment between

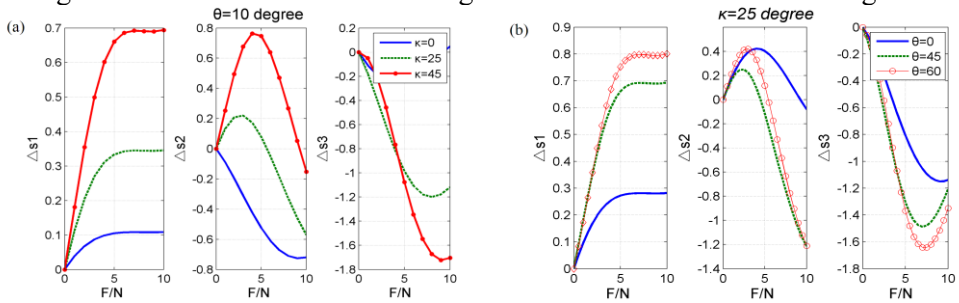

Fig. 2. (a) Simulated results for different ellipse angles κ at θ=10° (b) simulated results for different azimuth angles at κ=30° .

grating and PC controller and another segment between grating and polarization detector. That is illustrated in Fig .3 in section 3. Therefore, by the directions of simulations, the experiments will give practical performance.

3. Experiment and discussion

We will now describe our experimental set-up and present some experimental results that we have obtained to validate our numerical analysis. The schematic of the experiment setup is illustrated in Fig. 3. The input light from a tunable laser source (Agilent 8163B lightwave Multimeter) was launched into FBG. A 3-paddle fiber polarization controller (PC) was used to modify the polarization state of the light. The transmitted signal from FBG was directed into a polarization detector (General Photonics's in-line polarimeter POD-15-SS-02) which measured the Stokes parameters at a certain wavelength. After A/D conversion and signal process the experimental results were displayed and recorded in a computer.

During the measurements, the FBG was not strained and the ambient temperature was kept constant. Moreover, the fiber connectors were fixed to avoid polarization instability. The length of fiber grating is 10 mm and was placed parallel to a balance reference fiber.

For the 3-paddle fiber PC used to change the incident SOP, the second circle works as a $\lambda/2$ wave plate to alter azimuth angle (θ) and the first or third circle works as a $\lambda/4$ wave plate to alter ellipse angles (κ) of incident light.

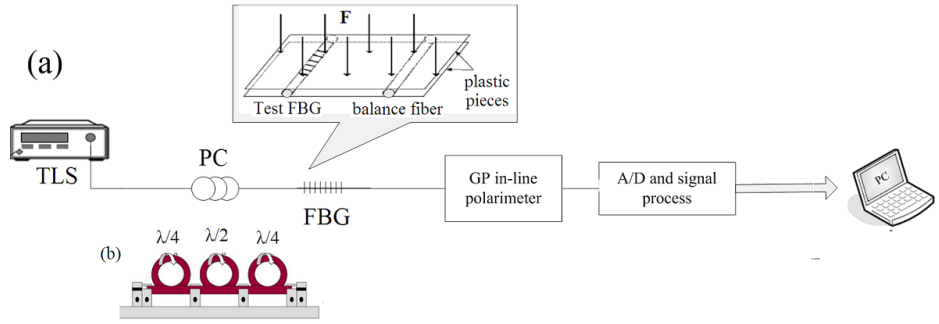

Fig. 3 (a) Experimental set-up. (b) 3-paddle fiber polarization controller.

3.1. Real-time measurement under different incident SOP

Firstly we applied a mobile telephone (Iphone 6 plus) to FBG and set it to vibrate mode to verify the performance of real-time measurement under different incident SOP. SOP of incident light was changed by adjusting PC for four cases randomly. The experimental results were recorded in Fig. 4(a) which depicts the evolutions of the four cases. It can be seen that all of the Stokes parameters can respond to the vibration of phone. The Stokes parameters present lowest sensitivity for the first case and highest sensitivity for the second case, which was enlarged as shown in Fig. 4(b) for example. The period is about 4.5ms, meaning a vibration frequency of about 222 Hz. So it is demonstrated that incident SOP has great influence on the performance of system.

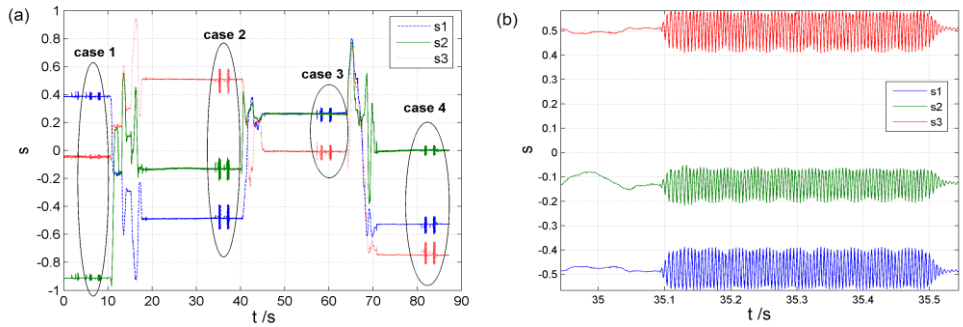

Fig.4 (a) Experimental evolutions of Stokes parameters response to a vibrated phone and (b) the enlarged responded curve for the second case.

3.2. Effect of azimuth angle and ellipse angle

Next we will adjust the 3-paddle fiber PC steadily to observe the influences.

a) Adjusting azimuth angle

The second paddle of PC was rotated from 0 ° to 180 °, stepped by 45° to alter azimuth angle, with the first and third circle fixed. It is should be noted that these angels are just the rotated angle of the second paddle, not the values of azimuth angle.

For each case, the force to be measured was applied to the FBG by placing weights on a plastic piece against the fiber. The weight applied was increased gradually from 0 to 800g, stepped by 200g. Experimental results were recorded and saved.

Fig. 5 (a) and (b) shows the experimental evolutions of three Stokes parameters during the process of placing weights when the second paddle of PC was rotated to 90° and 135°, respectively. It can be seen that s_1, s_2 and s_3 changes as applied weight increases while presents different sensitivity and linear range.

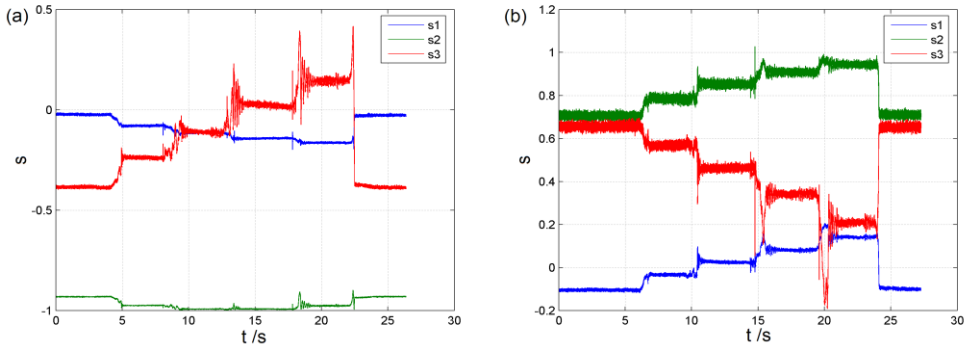

Fig.5 (a) Experimental evolutions of three Stokes parameters during the process of placing weights when the second paddle of PC (λ/2 wave plate) was rotated to (a) 90° and (b) 135°.

The amplitude of s_1, s_2 and s_3 under different amount of applied weights are recorded and used to depict the experimental performance curves. Fig. 6 (a), (b) and (c) are the amplitude changes versus weight amount under different rotated angle (that means different azimuth angles of SOP) for s_1, s_2 and s_3, respectively. It is found certainly that the difference of azimuth angle brings different characteristics. In some cases, non-linear property in range of 0-800g are presented, which also agrees with simulations, for example, rotated angel of 45° and 90° for s_2. The data with highest sensitivity are linearly fitted for each Stokes parameter, as shown in Fig. 6. The sensitivity of 0.3525/kgf, 0.5475/kgf, and -0.685/kgf are obtained for s_1, s_2 and s_3, respectively.

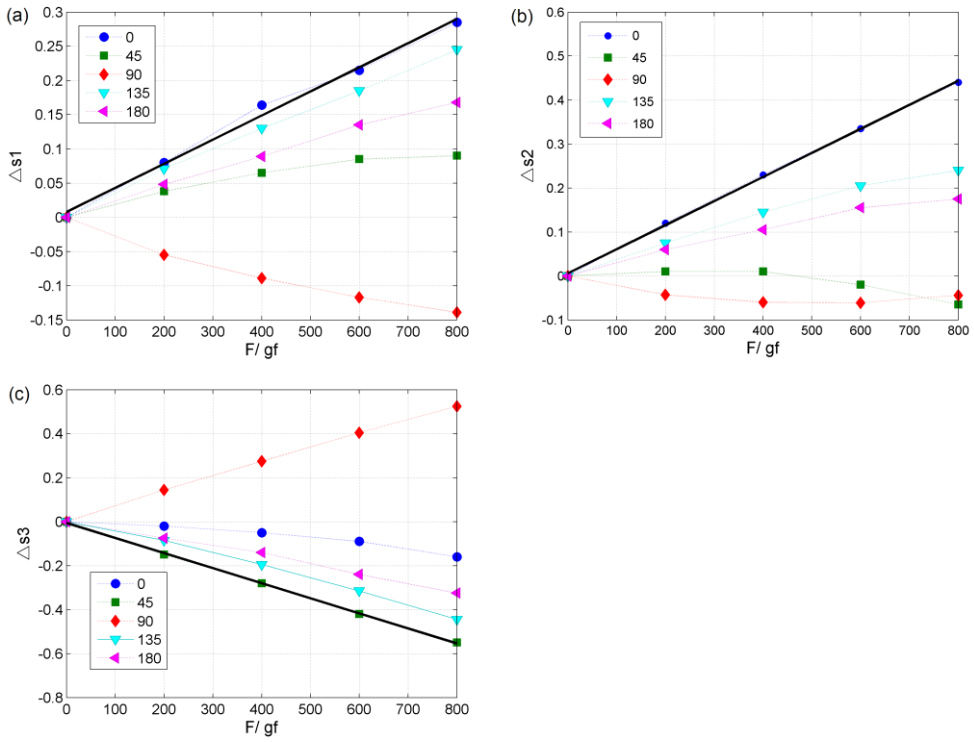

Fig. 6 The amplitude changes of Stokes parameters versus weight amount under different rotated angle of $\lambda/2$ wave plate for (a)s_1, (b)s_2 and (c)s_3..

（b）Adjusting ellipticity angle

Next the third paddle ($\lambda/4$ wave plate) of PC was rotated from 0° to 180°, stepped by 45° to alter ellipse angle, with the first and second paddles fixed.

Fig. 7 (a) and (b) depicts the experimental evolutions of three Stokes parameters during the process of placing weights when the third paddle of PC was rotated to 45° and 180°, respectively. It can be seen that for 180° case, s_3 presents very high sensitivity.

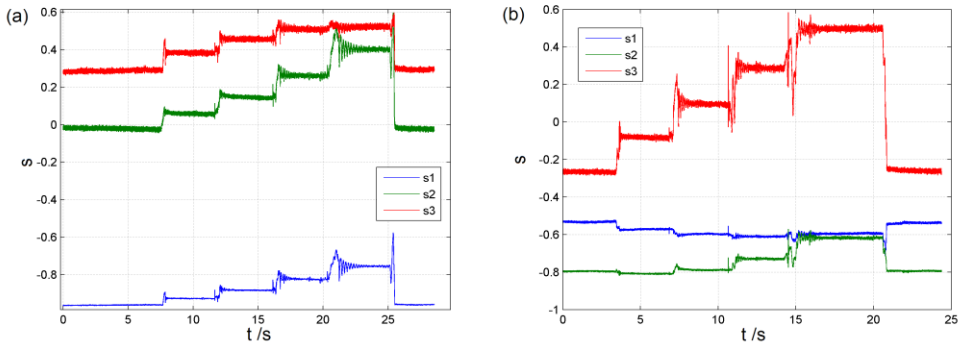

Fig. 7 Experimental evolutions of three Stokes parameters during the process of placing weights when the third paddle of PC (λ/4 wave plate) was rotated to (a) 90° and (b)180°.

Using the same method, the amplitude of s_1, s_2 and s_3 under different amount of applied weights are recorded and used to depict the experimental performance curves. Fig. 8(a), (b) and (c) are the amplitude changes versus weight amount under different rotated angles of λ/4 wave plate for s_1, s_2

and s_3, respectively. The data with highest sensitivity are linearly fitted, and the sensitivity of 0.2635/kgf， 0.52/kgf， 0.9475/kgf are obtained for s_1, s_2 and s_3, respectively.

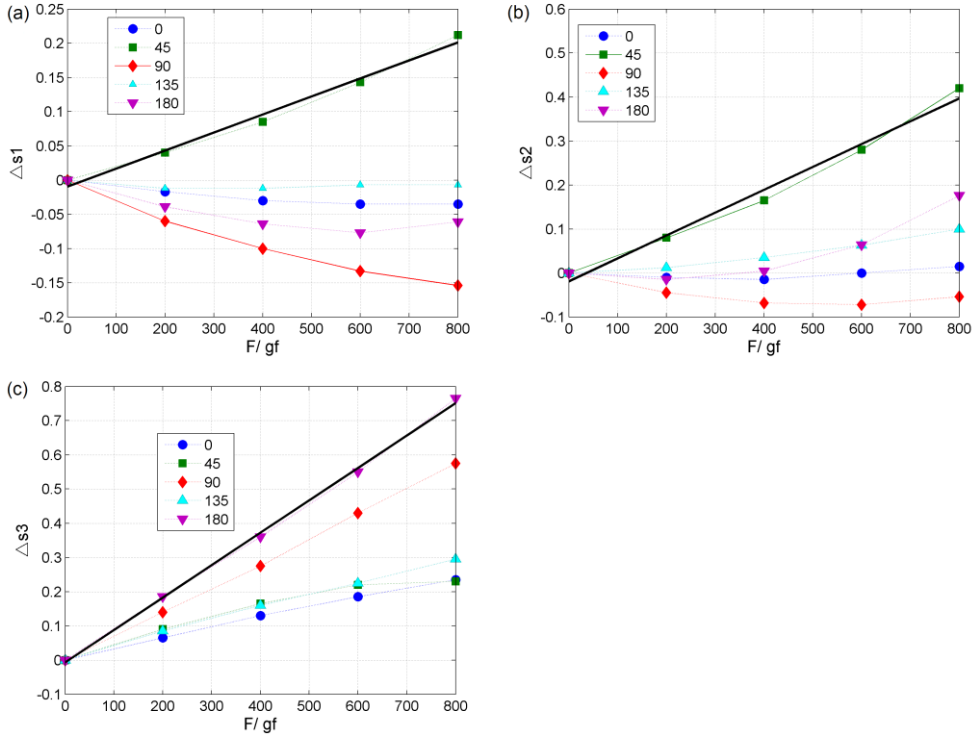

Fig. 8 The amplitude changes of Stokes parameters versus weight amount under different rotated angle of λ/4 wave plate for (a)s_1， (b)s_2 and (c)s_3.

4. Discussion and conclusion

Stokes parameters amplitude can be advantageously used to obtain transverse force measurements with uniform FBGs written into standard single mode fiber. In this paper the influences of incident SOP on the performance of sensor system are found by simulations. A 3-paddle fiber polarization controller was used in the experiment to adjust the azimuth angle and ellipse angle of the light. The experimental results show the great influences of incident SOP on the sensitivity and linear range, which is well agreed with the theoretical prediction. Although the 3-paddle fiber PC is a rough device, a satisfying response still can be found by adjusting PC steadily. In the experiments, a highest sensitivity of 0.9475/kgf was obtained with good linearity. Therefore this work offers new theories and simple method for transversal force sensing to improve the performance.

5. Acknowledgments

This work was supported by the Natural Science Foundation of Jiangsu Province (BK20161471) and Natural National Science Foundation of China (NSFC) (61371121).

6. References and Links

[1] A.D. Kersey, M.A. Davis, H.J. Patrick, M. LeBlanc, K.P. Koo, C.G.Askins, M.A.Putnam, and E.J.Friebele, “Fiber grating sensors”, J. Lightwave. Technol. **15**(8), 1442–1463 (1997).
[2] K.O. Hill and G. Meltz, “Fiber Bragg grating technology fundamental and overview,” J. Lightwave. Technol. **15**(8), 1263–1276 (1997).

[3] I. Abe, O. Fraz ão, M.W. Schiller, R. N. Nogueira, H. J. Kalinowski, and J. L. Pinto, "Bragg gratings in normal and reduced diameter high birefringence fiber optics," Meas. Sci. Technol. **17**(6), 1477(2006).
[4] Y. Wang, N. Chen, B. Yun, Z. Wang, C. Lu, and Y. Cui, "Effects of distributed birefringence on fiber Bragg grating under non-uniform transverse load," Opt. & Laser Technol. **40**(8), 1037-1040(2008).
[5] R. B. Wagreich, W. A. Altia, H. Singh, and J. S. Sirkis, "Effects of diametric load on fiber Bragg gratings in low birefringence fiber," Electron. Lett. **32**(13), 1223–1224(1996).
[6] R. Gafsi and M.A.E. Sherif, "Analysis of induced-birefringence effects on fiber Bragg gratings," Opt. Fiber Technol. **6**(3), 299-323(2000).
[7] F. Descamps, C. Caucheteur, P. M égret, and S. Bette , "Distribution profiling of a transverse load using the DGD spectrum of chirped FBGs," Opt. Express **23**(14), 18203-18217(2015).
[8] C. Caucheteur, S. Bette, R. Garc á-Olcina, M. Wuilpart, S. Sales, J. Capmany, and P. M égret, "Transverse strain measurements using the birefringence effect in fiber Bragg grating," IEEE Photon. Technol. Lett. **19**(13), 966–968(2007).
[9] C. Caucheteur, S.Bette, R. Garc á-Olcina, M. Wuilpart, S. Sales, J. Capmany, and P. M égret, "Influence of the grating parameters on the polarization properties of fiber Bragg gratings ," J. Lightwave Technol. **27**(8), 1000–1010 (2009).
[10] Y. Qiu, Q. Wang, H. Zhao, J. Chen, and Y. Wang, "Review on composite structural health monitoring based on fiber Bragg grating sensing principle," J. Shanghai Jiaotong University **18**(2), 129–139 (2013).
[11] N. Lammens, D. Kinet, K. Chah, G. Luyckx, C. Caucheteur, J. Degrieck, and P. M égret, "Residual strain monitoring of out-of autoclave cured parts by use of polarisation dependent loss measurements in embedded optical fiber Bragg gratings," Composites, Part A **52**, 38–44 (2013).
[12] L. Mohanty, S. C. Tjin, D. T. T. Lie, S. E. C. Panganiban, and P. K. H. Chow, "Fiber grating sensor for pressure mapping during total knee arthroplasty," Sens. Actuators, A **135**(2), 323–328 (2007).
[13] Y. Park, K. Chau, R. J. Black, and M. R. Cutkosky, "Force sensing robot fingers using embedded fiber Bragggrating sensors and shape deposition manufacturing," *in Proceedings of IEEE International Conference onRobotics and Automation* (IEEE, 2007), pp. 1510–1516.
[14] Yang Su, Yong Zhu, Baofu Zhang, and Hua Zhou，"Real-time transverse force sensing using fiber Bragg grating through direct Stokes parameters measurement"，Optics Express, **23**(25),32300(2015)
[15] J. Espejo and S. D. Dyer, "Transverse-stress fiber Bragg grating sensor with high spatial resolution and temperature stability," J. Lightwave Technol. **25**(7), 1777–1785(2007).
[16] Erdogan, "Fiber grating spectra," J. Lightwave Technol. **15**(8), 1277–1294(1997